RAMAIAH ISSN (Print) : 0975-7988

MS RAMAIAH MANAGEMENT REVIEW
July - December 2023, Vol 14(02), 1 – 11
DOI: 10.52184/msrmr.v14i02.000

Experimental Investigation of Fused Deposition Modelling Process Parameters to Optimize the Fabrication of Connecting Rod Bush

S V Nithesh, K T Imayan, and B. N. Sreeharan

Department of Mechanical Engineering, Kumaraguru College of Technology, Coimbatore, India

Article Type: Article

Article Citation: S V Nithesh, K T Imayan, and B. N. Sreeharan, Experimental Investigation of Fused Deposition Modelling Process Parameters to Optimize the Fabrication of Connecting Rod Bush. M.S. Ramaiah Management Review. 2023; 14(02), 1-11. DOI: 10.52184/msrmr.v14i02.000

Received date: November 31, 2023

Accepted date: December 15, 2023

***Author for correspondence:** S V Nithesh Department of Mechanical Engineering, Kumaraguru College of Technology, Coimbatore, India

Abstract

This paper describes the experimental investigation and optimization of various parameters affecting Fused Deposition modelling (FDM) Techniques, namely orientation angle, layer thickness, and nozzle diameter, to achieve finest surface texture values on 3D printed Acrylonitrile Butadiene Styrene (ABS) used to fabricate a connecting rod bush. The printer utilized here is ""Ultimaker 2+," and the filament is 2.85 mm in diameter and yellow. A Mitutoyo surface finish meter, an exceedingly accurate and precise measuring equipment, is used to determine surface finish. Taguchi's orthogonal array method is utilized to develop and conduct the experiments. The process parameters that affect the surface finish values of FDM printed models were then researched and optimized using a response table.

Keywords: Additive Manufacturing, Fused Deposition Modelling, Process Parameter Optimization, Taguchi, DEAR Algorithm

1. Introduction

In the industry, 3D printing is universally referred to as Additive Layer Manufacturing (ALM) or naively Additive Manufacturing (AM). These methods are typically computer-controlled. They make 3D products by depositing the necessary materials in the shape of layers that are layered one on top of the other. 3D-printers that use Fused Deposition Modelling technology may manufacture items with different layer thicknesses. This layer thickness influences print time and surface finish. The more the thickness, the better the surface finishes, but the longer the print time. As the layer thickness increases, the surface quality decreases, but the printing speed improves. Friction and surface wear qualities are intimately connected to surface roughness. Higher Ra surfaces often have slightly higher friction and wear down faster. Shape and ripple (amplitude and frequency) must also be taken into account. It is often stated using the degree of deviation as well as the direction of the reference surface to the normal vector associated with the perfect shape. When there are considerable variations, surface becomes irregular. If the variations are minor, the surface is

even. The roughness of everyday practical things and their interactions with their surroundings has a significant impact. Based on tribology, rough surfaces have a large coefficient of friction and wear quicker than smooth surfaces. The roughness is also a useful indicator for the smooth operation of mechanical parts since surface defects can act as catalysts for rust and corrosion. Roughness, on the other hand, may be a reason for encouraging adherence. Surface fractality, is a cross-scale descriptor which results in more accurate forecasts of mechanical interactions at surfaces. The surfaces may be contact in stiffness and stiction.

Even though high roughness levels are generally undesired, they might be costly and difficult to control during the manufacturing process. Managing the surface texture of FDM parts, in particular, will be difficult and costly.

Surface finish reduction frequently raises manufacturing costs. This frequently reduces the component's performance in the application as well as its production cost. The surface structure is critical for controlling contact dynamics. When it comes to machined surfaces, roughness is regarded detrimental to the performance of an object. As a result, the majority of production prints have an upper but not a lower roughness limit.

ABS, the proposed material for the connecting rod bush, offers good impact resistance and structural rigidity. It is also resistant to high and low temperatures and has great electrical insulation. Its high rigidity, chemical resistance, and abrasion resistance are just a few of the characteristics that make it excellent for various applications. ABS material is not advised for use in high-temperature environments due to its low melting point. Since ABS has low melting point, it is simple to create using home 3D printers and injection moulding procedures.

ABS comes in long filaments wound on spools for usage in 3D FDM printers. They are fed into an extrusion head, which melts and liquefies the ABS. Once it has transformed into a liquid state, whether through heating or not, the material is utilized to construct the platform layer by layer.

2. Literature Review

Several investigators have recently studied the impact of different 3D printing process factors on enhancing the quality of components manufactured using FDM, shortening the production process, and improving their mechanical properties. The main objective of the related investigation was to evaluate the dimensional precision, production time, and tensile strength of ABS components 3D printed using FDM technology, while incorporating different printed surfaces and orientation angles.

In their investigation, Zhai et al. [1] discovered the influence of surface configuration on conventional contact stiffness. The study shows that for a material, the interpreter of the power law connection is highly dependent on fractal size and RMS slope, whereas the friction coefficient is heavily influenced by RMS roughness. Dinesh Yadav et al. [2] used ANFIS to model and analyze crucial process parameters of an FDM 3D-printer. They concluded that as layer thickness grows, the % of errors reduces.

Wang et al.'s [3] investigation of the anisotropic behavior of 3D-printed materials and its effects on their tensile properties found that (i) anisotropy increases as strain rate decreases, and (ii) tensile fracture

occurring in vertical plane exhibits a high significant level of identity than one occurring in a parallel plane. Mohammad Taufik et al. [4] conducted research on the build edge shape for surface quality projection in fused deposition modelling (FDM). The build edge characteristics for FDM parts are found to be significantly diverse from one another for various building orientation ranges.

Yan et al. [5] presented a review of fast prototyping methods and systems in this paper. This was based on the quick and affordable fabrication of complex-surfaced patterns and moulds. They concluded by stating that a decision might be made based on factors such as the product's qualities, the time it takes to print, how effectively it prints, and rapid prototyping. Griffiths et al. [6] utilizing the Design of Experiments (DoE) method to enhance the tensile property and notched bending characteristics of FDM components. They obtained the outcome for a variety of factors, including material kind, cost-effectiveness, and layer height.

Farina et al.'s [7] examination of the hardness and bending strength of 3D-printed composite materials with fractal form led to the finding that fractal geometry reinforcements increased both the strength of crack and remaining load. Fracture was prevented upon the application of force due to the interlock between the matrix and reinforcing ribs. In terms of material development, Roberson et al. [8] addressed the increasing application of FDM-type technologies. They presented a comprehensive review of the applications of electromagnetic and electrochemical technologies. Finally, they demonstrated how 3D printable materials for future applications are being developed.

In their study, Chohan et al. [9] the Taguchi orthogonal arrays and genetic algorithms were employed to optimize the Fused Deposition Modeling (FDM) printing process parameters for achieving improved surface finish, thickness control, and external dimensions of ABS polymer specimens. They came to the conclusion that nozzle speed affects surface finish in ABS, with lower nozzle speeds producing superior surface quality. Tran et al. [10] engaged in a study involving 3D printing of biomaterials and the quantitative assessment of structural components inspired by nature, evaluating their performance under both in-plane and transverse loads. Finally, when selecting a material, it was discovered that adhesive and cohesive layers both contribute in absorbing the energy imparted by a shockwave.

Surface roughness and energy usage were both taken into consideration by Peng and Yan [11]. Definable structures were printed on three separate printers after various parameters, including infill ratio, essential process variables, printing speed, and layer thickness, were changed. According to this study, the component most responsible for a superior surface finish is layer thickness. The performance of the surface finish on printed products created by an FDM 3D printer using PLA+ material is specifically indicated as being affected by direction in the study of Alsoufi et al. [12]. They have offered three distinct graphical representations of the surface texture profile. They came to the conclusion that for improved surface quality, the layer height must be kept as low as possible.

Mishra et al.'s [13] research used chemical misting to provide their experimental evaluation of FDM-built items. They have selected several criteria and gone through the manufacture technique with their levels. They concluded that surface finish has the greatest impact on the air gaps

and the least impact on the other metrics. According to Pérez et al.'s research [14], critical elements such as material extrusion, chamber, extruder, and deposition qualities form the foundation for improved surface quality in Fused Deposition Modelling (FDM). They separated it into phases and ran experiments to achieve the optimal surface smoothness. They concluded that the performance of printed materials is mostly determined by the printing settings used, and they recommended using a lesser value for layer height.

Kovan et al. [15] explored how printing parameters impact the surface properties of 3D-printed PLA products. They came to the conclusion that print time varies according to printer type, component dimension, and layer thickness. In this case, the layer thickness is more crucial than other factors. Novakova-Marcincinova and Novak-Marcincin [16] confirmed and verified the structural characteristics of the ABS plastics to be used in the FDM quick prototyping technique. They prioritized the optimization of FDM printed samples over alternative possibilities. The conclusion explains how to choose criteria depending on how materials, quantity of goods, quality, and economic considerations interact.

In FDM-generated samples, Luanin et al.'s [17] examined how layer thickness, deposition angle, and infill density influenced the maximum flexural force. They concluded that layer thickness had the greatest impact on flexural force after considering the features of layer thickness, deposition angle, and infill. The 3D printing of textile-based architectures using FDM and various polymer materials is described by Melnikova et al. in [18]. They reported their findings after considering a wide range of conditional criteria. They got to this conclusion after discovering that ABS is delicate for component models and that hard PLA and nylon are used in the textile industry.

Applying Taguchi method with desirability approach, Camposeco-Negrete [19] presented a research aimed at optimizing FDM parameters to enhance component durability, efficiency, and the sustainability of the process. They considered variables such as printing plane, orientation angle, filling pattern, and layer thickness. When using the Taguchi approach, four of the six variables gave a better result, resulting in a conclusion. Samykano et al. [20] investigated the mechanical and physical properties of FDM-produced ABS: impact of printing parameters. Based on variables like infill%, raster angle, and layer thickness, they offered information on the tensile qualities and implications for the mechanical properties of FDM specimens.

In their research on the mathematical analysis of surface quality for vapor treatment of ABS parts produced using FDM, Chohan et al. [21] published their findings. Regarding vapour smoothing and 3D-printed items, they utilized Taguchi and ANOVA. Six parameters were investigated, and it was discovered that the surface polish improves after numerous vapor smoothing cycles. Due to its inexpensive cost and characteristics that allow metal implants to maintain the environment over time, such as raster angle and air gaps, nickel was selected as a coating material in Khan et al.'s [22] study. They came to the conclusion that this process improved each element's surface polish.

Umaras et al. [23] provided information on additive manufacturing based on geometric correctness and affecting factors. It highlighted how additive manufacturing makes geometrical correctness difficult to obtain. Tekinalp et al. [24] used additive

manufacturing to perform research on highly orientated carbon fiber polymer composites based on their parameter selection. The FDM technology later proved to be capable of printing highly aligned carbon fibers. In their work, Yeshwanth et al. [25] employed a wide range of materials for manufacturing purposes. He also took into account the weight and cost in order to lower the respective metrics. He employed the DEAR algorithm to identify an appropriate material for the welding fixture.

3. Methodology

A total of nine samples were 3D printed and analyzed to investigate the impact of process variables such as nozzle diameter, orientation angle, and layer thickness on surface quality values. The three factors chosen for further investigation determine the surface finish value of ABS in the FDM process. The Taguchi L9 orthogonal array technique was used to organize and carry out the trials. The values of the parameters utilized to conduct the experiments are listed in Table 1. Table 2 shows the L9 orthogonal experimental design with process parameters.

TABLE 1. Values of process parameters.

Parameters	Types	1	2	3
Layer thickness (mm)	A	0.1	0.2	0.3
Orientation angle (degree)	B	0	15	30
Nozzle Diameter (mm)	C	0.4	0.6	0.5

TABLE 2. Randomly chosen run table.

A	B	C	Original run	Actual run
0.1	0	0.4	1	1
0.1	15	0.6	2	3
0.1	30	0.8	3	8
0.2	0	0.6	4	2
0.2	15	0.8	5	6
0.2	30	0.4	6	7
0.3	0	0.8	7	4
0.3	15	0.4	8	5
0.3	30	0.6	9	9

The printer used for 3D printing is an Ultimaker 2+, and the material is 2.85 mm diameter yellow ABS filament. The filament is strong and durable, with high dimensional stability and impact resistance and the capacity to withstand temperatures of up to 85 °C. The SolidWorks 3D model in Figure 1 was exported to STL format before being loaded into the Ultimaker Cura software and sliced to the desired layer thickness before being delivered to the printer via SD card.

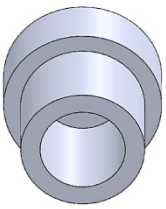

FIGURE 1. Connecting rod bush.

The printing speed is kept constant at 40 mm/s, which is considered the minimum speed for a good finish; the infill pattern is line type with a density of 60%; and the support structure is auto-selected by the software. Figure 2 depicts the entire set of 3D-printed connecting bushes.

FIGURE 2. 3D Printed parts.

The surface finish values of 3D printed objects were measured using a Mitutoyo digital surface finish tester, and the results were fairly precise. The nine 3D printed samples were held rigid in a V-fixture. The machine ensures the rigidity of the measuring platform. The surface finish tester is then held parallel to the fixture, the machine's skid is kept in contact with the sample, and the surface finish is measured. Each product was tested three times to ensure a good and precise measurement, and an average value was used. The surface finish is determined using a Mitutoyo surface finish meter, which is extremely exact and precise, as shown in Figure 3 concerning surface finish measurement.

FIGURE 3. Surface roughness testing process.

TABLE 3. Surface finish values measured.

Exp. no	Parameters A	B	C	Surface finish (RMS)
1	0.1	0	0.4	263.2
2	0.1	15	0.6	252
3	0.1	30	0.8	281.2
4	0.2	0	0.6	333.2
5	0.2	15	0.8	301.2
6	0.2	30	0.4	320.8
7	0.3	0	0.8	331.6
8	0.3	15	0.4	334.8
9	0.3	30	0.6	278.8

Table 3 represents the calculated surface finish values.

3.1. Coordinate Measuring Machine (CMM) Report

Dimensions of the specimen given as input which the outer diameter is 20 mm and inner diameter is 14 mm.

The CMM is used to determine the deviation created during printing by measuring the outer and inner diameters of the specimen. Table 4 shows the value of deviation obtained by subtracting the measured outer and inner diameter values from the designed outer and inner diameter values.

3.2. Ranking Method based on Data Envelopment Analysis

Weight fractions are not necessary when applying Data Envelopment Analysis-based Ranking (DEAR) method as developed by Charnes et al. in 1978. This method involved creating a ratio known as the Multi-Response Performance Index (MRPI) by mapping the initial set of responses. In order to identify the option that would be most useful given the options supplied, MRPI values were used. The following are the sequence of steps in performing DEAR algorithm:

TABLE 4. Deviation in diameter values.

S. No.	Surface finish (RMS)	Measured outer diameter (mm)	Deviation in outer diameter (mm)	Measured inner diameter (mm)	Deviation in inner diameter (mm)
1	263.2	20.412	0.412	13.858	0.142
2	252	20.390	0.390	13.896	0.104
3	281.2	20.401	0.401	13.861	0.139
4	333.2	20.387	0.387	13.913	0.087
5	301.2	20.488	0.4880	13.764	0.236
6	320.8	20.483	0.483	13.737	0.263
7	331.6	20.511	0.511	13.633	0.367
8	334.8	20.500	0.500	13.661	0.339
9	278.8	20.357	0.357	13.762	0.238

(1) Formation of alternate and objective matrix
(2) Computation of normalized value
(3) Calculation of Weighted Response
(4) Determination of the MRPI
(5) Ranking and determining the best alternative.

3.2.1. Formation of Alternate and Objective Matrix

This is the first stage in the DEAR method, and the matrix consists of "i" and "j," with "i" denoting the number of choices and "j" representing the quantity of objectives. The Oij matrix is formed as a result, with i taking the values (i = 0,1,2,3,...,ni) and j taking the values (j = 0,1,2,3,...,nj).

3.2.2. Computation of Normalized Value

The method of normalising the maximization and minimization criteria of the parameters chosen follows. To maximize, divide the particular value by the sum of their objective values to obtain the Normalized value (Nij), as shown in equation (1). To minimize, reduce the reciprocal of the specific value by its reciprocated objective value to obtain the Normalized value (Nij), as shown in equation (2).

$$Nij = \frac{Oij}{\sum_{i=n}^{ns} Oij} \tag{1}$$

$$Nij = \frac{1/Oij}{\sum_{i=1}^{ns} 1/Oij} \tag{2}$$

3.2.3. Calculation of Weighted Response

The multiplication of the respective objective matrix and the normalized matrix gives the value of the weight response, which is given in equation (3).

$$Aij = Oij * Nij \tag{3}$$

3.2.4. Determination of the MRPI

The ratio of the summation of the maximized objective (Wmxi) to that of the minimized objective (Wmmi) gives the value of MRPI, which is given in equation (6).

$$Wmxi = \sum_{j=1}^{max} Aij \tag{4}$$

$$Wmmi = \sum_{j=1}^{min} Aij \quad (5)$$

$$MRPI\left(R_i\right) = \frac{W_{mxi}}{W_{mmi}} \quad (6)$$

3.2.5. Ranking and Determining the Best Alternative

The MRPI scores were computed and ranked. The analysis was performed using the given MRPI values to obtain the outcome of the best-optimized specimen.

The values were documented and included in the calculation using the methods outlined above. To begin, the Oij and its inverse values were tabulated and substituted in order to obtain the normalized matrix. Because the specimen's surface finish value should be high, it is substituted in the maximization formula, whereas the deviation in the inner and outer diameters of the specimen should be minimal, so it is substituted in the minimization formula, and separate normalized values are obtained.

Weighted response (Aij) values are calculated using equation (3) and tabulated. Now, the total of the Aij values of surface finish yields the value of maximum objective summation (Wmxi), and the sum of the Aij values of both inner and outer diameters yields the value of minimum objective summation (Wmmi). Based on which the MRPI value is determined.

TABLE 5. MRPI values.

Specimen no	W_{max} (mm)	W_{min} (mm)	MRPI (mm)
1	25.6876	0.06652	386.19
2	23.5479	0.06652	354.022
3	29.3212	0.06652	440.819
4	41.1681	0.06652	618.927
5	33.6404	0.06652	505.754
6	38.161	0.06652	573.717
7	40.7737	0.06652	612.997
8	41.5645	0.06652	624.885
9	28.8228	0.06652	433.326

Table 5 shows the values of maximized and minimized objectives using the equations (4) and (5). MRPI value is calculated with the obtained values using equation (6).

3. Results and Discussions

The layer height should not be larger than 80% of the nozzle diameter, according to the associated standard. The maximum layer height with a standard 0.4 mm nozzle is roughly 0.32 mm. Layer heights of up to 0.48 mm can be reached using a 0.6 mm nozzle. The parameters are independent with all of these constraints. Individually adjusting the settings may have a different result. As a result, the nozzle diameter may be considered to be responsible for the overall quality of the product; that is, the smaller the nozzle size, the better the finish. Because the layer height represents the level of details on the printed objects (both flat and inclined surfaces), it can be claimed that the layer height is important for achieving a good surface finish.

TABLE 6. Rank values.

Specimen no	MRPI (mm)	Rank
1	386.19	8
2	354.022	9
3	440.819	6
4	618.927	2
5	505.754	5
6	573.717	4
7	612.997	3
8	624.885	1
9	433.326	7

The rank of the MRPI values is obtained by using the DEAR algorithm, to determine the optimized specimen. Here, Table 6 shows that specimen no. 8 holds the 1st rank, so it was considered the optimized specimen.

TABLE 7. Optimized process parameters.

Parameters	Layer thickness	Orientation angle	Nozzle diameter
Result	0.1	30	0.6

Validation experiments were conducted using the above process parameters to ascertain them. The results of the process parameters used to obtain the best specimen are tabulated in Table 7.

TABLE 8. Validation results.

Parameters	Layer thickness	Orientation angle	Nozzle diameter	RMS Value
Result	0.1	30	0.6	334.8

The surface finish value for the specimen with the resulting process parameter is finalized in Table 8.

TABLE 9. Optimized result.

Parameters	RMS	Outer diameter deviation	Inner diameter deviation
Result	334.8	0.5	0.339

Based on the result obtained using the DEAR algorithm, the values of deviation obtained using CMM are listed in Table 9.

4. Conclusions

Additive manufacturing is one of the most extensively used 3D printing processes, and diverse parts are made on a regular basis utilising FDM technology. This study was conducted to determine the most efficient method of creating FDM parts. The main advantage of this technology is that the parts can be easily produced using a wide range of inexpensive, non-toxic ingredients and equipment. Using the Taguchi L9 Orthogonal array, this paper studied the relevance of layer thickness, orientation angle, and nozzle diameter on the surface finish attributes of FDM-printed ABS samples, as well as the individual parametric effects on process features. Layer height should not be larger than 80% of the nozzle diameter to get a better surface finish value, which is the primary goal of this research work. The level of detail on the printed objects is represented by the layer height. That is, as the nozzle height decreases, the deviations and surface roughness decrease, resulting in a better surface quality. It is necessary to optimize the nozzle diameter to minimize the deviations caused in the product. Based on the findings, it is feasible to conclude that surface roughness gets affected by the layer thickness in 3D printing. The surface finish of FDM-printed ABS samples is only slightly affected by the orientation angle and nozzle thickness. To summarize, because FDM is a parameter-dependent process, surface properties are heavily influenced by parameter selection, which is in turn influenced by the individual applications.

References

1. Zhai, C., Gan, Y., Hanaor, D., Proust, G., & Retraint, D. (2016). The role of surface structure in normal contact stiffness. *Experimental Mechanics*, 56, 359–368. doi:10.1007/s11340-015-0107-0.S2CID 51901180

2. Yadav, D, Chhabra, D, Gupta, R. K, Phogat, A, & Ahlawat, A. (2020). Modeling and analysis of significant process parameters of FDM 3D printer using ANFIS, *Materials Today Proceedings*, 21, 1592–1604. doi:10.1016/j.matpr.2019.11.227
3. Wang, Y., Li, X., Chen, Y., & Zhang, C, (2021) Strain rate dependent mechanical properties of 3D printed polymer materials using the DLP technique, *Additive Manufacturing*, 47, Article ID 102368. doi:10.1016/j.addma.2021.102368
4. Taufik, M., Jain, P. K. (2016). A study of build edge profile for prediction of surface roughness in fused deposition modeling. *Journal of Manufacturing Science and Engineering*. 138. doi:10.1115/1.4032193
5. Yan, X., Gu, P. (1996). A review of rapid prototyping technologies and systems. *Computer-Aided Design and Applications*, 28, 307–318. doi:10.1016/0010-4485(95)00035-6
6. Griffiths, C.A., Howarth, J., De Almeida-Rowbotham, G., Rees, A. (2016) A design of experiment approaches to optimize tensile and notched bending properties of fused deposition modeling parts. Proceedings of the **Institution** of **Mechanical** Engineers, **Part B**: Journal of **Engineering Manufacture**, 230, 1502–1512. doi:10.1177/0954405416640182
7. Farina, I., Goodall, R., Hernandez-Nava, R., di Filippo, A., ´Colangelo, F., and Fraternali, F. (2019). Design, microstructure and mechanical characterization of Ti6Al4V reinforcing elements for cement composites with fractal architecture. Materials & Design, 172, Article ID 107758. doi:10.1016/j.matdes.20.19.107758
8. Roberson, D., et al. (2015). Expanding the applicability of FDM-type technologies through materials development. *Rapid Prototyping Journal*, 21, 137–143. doi:10.1108/rpj-12-2014-0165
9. Chohan, J. S., Kumar, R., Yadav, A., Chauhan, P., Singh, S., Sharma, S., ... & Rajkumar, S. (2022). Optimization of FDM printing process parameters on surface finish, thickness, and outer dimension with abs polymer specimens using Taguchi orthogonal array and genetic algorithms. *Mathematical Problems in Engineering*, 2022. doi:10.1155/2022/2698845
10. Tran, P., et al. (2017). Bi-material 3D printing and numerical analysis of bio-inspired composite structures under in-plane and transverse loadings. *Composites Part B: Engineering*, 108, 210–223. doi:10.1016/j.compositesb.2016.09.083
11. Peng, T., & Yan, F. (2018). Dual-objective analysis for desktop FDM printers: energy consumption and surface roughness. *Procedia CIRP*, 69, 106–111. doi:10.1016/j.procir.2017.11.084
12. Alsoufi, M. S., & Elsayed, A. E. (2017). How surface roughness performance of printed parts manufactured by desktop FDM 3D printer with PLA+ is influenced by measuring direction. *American Journal of Mechanical Engineering*, 5, 211–222. doi:10.12691/ajme-5-5-4
13. Mishra, S. B., Acharya, E., Banerjee, D., & Khan, M. S. (2019). An experimental investigation of surface roughness of FDM build parts by Chemical Misting. In IOP Conference Series: Materials Science and Engineering (Vol. 653, No. 1, p. 012043). IOP Publishing. doi:10.1088/1757-899X/653/1/012043.
14. Pérez, M., Medina-Sánchez, G., García-Collado, A., Gupta, M., & Carou, D. (2018). Surface quality enhancement of fused deposition modeling (FDM) printed samples based on the selection of critical printing parameters. Materials, 11, 1382. doi:10.3390/ma11081382
15. Kovan, V., Tezel, T., Topal, E. S., & Camurlu, H. E. (2018). Printing parameters effect on surface characteristics of 3D printed PLA materials. *Machines Technologies Materials*, 12, 266–269.
16. Novakova-Marcincinova, L., & Novak-Marcincin, J. (2013). Verification of mechanical properties of abs materials used in FDM

rapid prototyping technology. *Proceedings in Manufacturing Systems*, 8, 87–92.

17. Lužanin, O., Movrin, D., & Plančak, M. (2014). Effect of layer thickness, deposition angle, and infill on maximum flexural force in FDM-built specimens. *Journal for Technology of Plasticity*, 39, 49–58.
18. Melnikova, R., Ehrmann, A., & Finsterbusch, K. (2014). 3D printing of textile-based structures by Fused Deposition Modelling (FDM) with different polymer materials. *IOP Conference Series: Materials Science and Engineering*, 62(1), 012018. doi:10.1088/1757-899X/62/1/012018
19. Camposeco-Negrete, C. (2020). Optimization of FDM parameters for improving part quality, productivity and sustainability of the process using Taguchi methodology and desirability approach. *Progress in Additive Manufacturing*, 5(1), 59–65. doi:10.1007/s40964-020-00115-9
20. Samykano, M., Selvamani, S. K., Kadirgama, K., Ngui, W. K., Kanagaraj, G., & Sudhakar, K. (2019). Mechanical property of FDM printed ABS: influence of printing parameters. *The International Journal of Advanced Manufacturing Technology*, 102(9), 2779–2796. doi:10.1007/s00170-019-03313-0
21. Chohan J. S., Singh, R., & Boparai, K. S. (2016). Mathematical modelling of surface roughness for vapour processing of ABS parts fabricated with fused deposition modelling. *Journal of Manufacturing Processes*, 24, 161–169. doi:10.1016/j.jmapro.2016.09.002
22. Khan M. S., Mishra, S. B., Kumar, M. A., & Banerjee, D. (2018). Optimizing surface texture and coating thickness of nickel coated ABS-3D parts. *Materials Today Proceedings*, 5, Article ID 19011. doi:10.1016/j.matpr.2018.06.252
23. Umaras, E., & Tsuzuki, M. S. (2017). Additive manufacturing-considerations on geometric accuracy and factors of influence. *IFAC-PapersOnLine*, 50, 14940–14945. doi:10.1016/j.ifacol.2017.08.2545
24. Tekinalp, H. L., Kunc, V., Velez-Garcia, G. M., Duty, C. E., Love, L. J., Naskar, A. K., ... & Ozcan, S. (2014). Highly oriented carbon fiber–polymer composites via additive manufacturing. *Composites Science and Technology*, 105, 144–150. doi:10.1016/j.compscitech.2014.10.009
25. Yashwanth, P., Kumaresh, T. B., Krishnakanth, C. K., Viswanath, M., & Sreeharan, B. N. (2022). Application of DEAR algorithm in selection of material for making a flexible fixture for ATV control arms. In AIP Conference Proceedings (Vol. 2446, No. 1, p. 180017). AIP Publishing LLC. doi:10.1063/5.0108345
26. Kishore, G., Rajeswaran, K. S., Mugunth, S., Raj, N. M., & Sreeharan, B. N. (2022). An investigation on selection and validation of suitable material to a roller of an automated solar panel cleaning system using DEAR algorithm. In AIP Conference Proceedings (Vol. 2446, No. 1, p. 110005). AIP Publishing LLC. doi:10.1063/5.0108389